Journal of Mining Science, Vol. 37, No. 5, 2001

ROCK FAILURE

DYNAMICS OF MICROFAILURES IN ELASTIC ZONE DURING EXPLOSION OF SPHERICAL CHARGE IN ROCK

E. N. Sher and N. I. Aleksandrova UDC 550.834

A calculated model is developed for explosion of spherical charge in rock; it takes into account accumulation of damages in the elastic zone under the action of blast wave. The condition, under which the density of generated microcracks reaches the critical value, is used as failure criterion. The microcrack growth rate is determined by exponential function of equivalent stress.

Explosion, rock, microfailure, damage accumulation, wave of shattering

Consider rock disturbance kinetics in the elastic zone of deformation of the rock mass being blasted. It is assumed that damages in the loaded solid body arise as a result of thermofluctuation processes. Such approach is developed in the theory of long-term strength [1].

The tests of various materials for tension showed that when the stress σ is constant, the time up to the sample failure decreases exponentially

$$\tau = t_0 \exp\left(-\frac{\sigma}{\sigma_0}\right). \tag{1}$$

Parameters t_0 and σ_0 of the dependence in question are found for many solid bodies.

The structural analysis of the bodies under load showed that generation, accumulation, and mergence of defects occur in them in course of time. Failure takes place when the defect density N reaches the critical value N_c. Assuming that microcracks appear with constant velocity if the tensile stress is assigned, from (1), we obtain

$$\dot{N} = \frac{N_c}{t_0} \exp\left(\frac{\sigma}{\sigma_0}\right). \tag{2}$$

Integration of this equation makes it possible to determine dynamics of microdefect accumulation when the tensile stress $\sigma(t)$ depends on time:

$$N(t) = \frac{N_c}{t_0} \int_0^t \exp\left(\frac{\sigma(t)}{\sigma_0}\right) dt. \tag{3}$$

Institute of Mining, Siberian Branch, Russian Academy of Sciences, Novosibirsk, Russia. Translated from Fiziko-Tekhnicheskie Problemy Razrabotki Poleznykh Iskopaemykh, No. 5, pp. 33–40, September-October, 2001. Original article submitted August 15, 2001.

1062-7391/01/3705-0475$25.00 ©2001 Plenum Publishing Corporation

In failing the elastic medium by explosion of spherical charge, the radial σ_r and tangential σ_θ stresses arise:

$$\sigma_r = -\frac{1}{r} f''(t-r) - 4\mu^2 \left[\frac{1}{r^2} f'(t-r) + \frac{1}{r^3} f(t-r)\right] - P,$$

$$\sigma_\theta = -\frac{1-2\mu^2}{r} f''(t-r) + 2\mu^2 \left[\frac{1}{r^2} f'(t-r) + \frac{1}{r^3} f(t-r)\right] - P. \quad (4)$$

Here, $f(\xi)$ is the elastic potential of deformation, $\mu^2 = 0.5(1-2\nu)/(1-\nu)$, ν is Poisson's ratio, and P is the rock pressure; the time t, the distance from the center of explosion r, and σ_r, σ_θ are presented in the dimensionless form. The initial charge radius a_0, the time a_0/c_p (c_p is the longitudinal wave velocity), and the compression modulus ρc_p^2 (ρ is the rock density) are taken as units of length, time, and stress, respectively.

In order to obtain a dependence similar to (3), in the case of biaxial stress state, it is required to find the expression of the effective stress $\sigma_f(t)$ determining the damage accumulation rate in terms of σ_r and σ_θ. The intensity of damage accumulation depends on the proximity of the point $(\sigma_r, \sigma_\theta)$ to the limit curve of failure C_f. Such curves (chart of rock strength) are plotted for many media by means of biaxial static tests of samples [2]. Their form can be approximately represented by piecewise-linear function (Fig. 1) symmetric about the straight line $\sigma_r = \sigma_\theta$. Here, the following strength criteria take place:

– uniaxial tension (section *I*)

$$\sigma_\theta = \sigma_t \quad (\text{if } \sigma_r > \sigma_\theta > 0);$$

– the Coulomb – Mohr condition (section *II*)

$$\sigma_\theta - \sigma_r \frac{\sigma_t}{\sigma_c} - \sigma_t = 0;$$

– the Tresca condition (section *III*)

$$\frac{\sigma_\theta - \sigma_r}{2} = \tau_p,$$

where σ_t, σ_c, and τ_p are the tensile, compressive, and shear strength, respectively. The parameters σ_t and σ_c are determined by uniaxial test, τ_p — by means of biaxial test. For some rocks, their values can be found in [2].

It follows from the theory of long-term strength that if the point characterizing the stress state of the medium element is within C_f, then the element failure can take much greater time than in the static tests; if the point in question is outside C_f, the time up to the failure considerably decreases. For this reason, the points of C_f are equivalent to each other and, in particular, to uniaxial tension by the stress σ_t; hence, in (3) this value can be taken as the effective stress $\sigma_f = \sigma(t) = \sigma_t$.

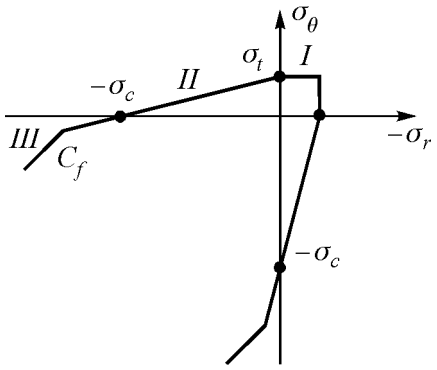

Fig. 1

For the arbitrary stress state, two types of σ_f were used in this paper. The first one is obtained as the value at the point of intersection of the axis $\sigma_r = 0$ and straight line passing through the point $(\sigma_r, \sigma_\theta)$ parallel to section *II* (Fig. 1)

$$\sigma_f = \sigma_\theta - \sigma_r \frac{\sigma_t}{\sigma_c}, \quad \sigma_r < 0. \tag{5}$$

Here, the points in the straight lines parallel to section *II* are equivalent, and the straight lines are the level curves for $\sigma_f(\sigma_r, \sigma_t)$. The variant under consideration is used for great τ_p when failure does not occur in section *III*.

In the second case, in the plane $(\sigma_r, \sigma_\theta)$, one-parametric family of curves similar to C_f was plotted by contraction with the coefficient α. If $\alpha < 1$, the limit curve passes to the elasticity domain; if $\alpha \geq 1$, it passes to the failure domain. Each point $(\sigma_r, \sigma_\theta)$ is in a certain curve of the family. Its proximity to the limit curve depends on the value of α. In this instance, it was assumed that $\sigma_f = \alpha\sigma_t$. Hence, when $\sigma_r < \sigma_\theta$:

$$\sigma_f = \sigma_\theta, \quad \text{if} \quad \sigma_r > 0,$$

$$\sigma_f = \sigma_\theta - \sigma_r \frac{\sigma_t}{\sigma_c}, \quad \text{if} \quad \sigma_r < 0, \quad \frac{\sigma_\theta}{\sigma_r} < \beta, \tag{6}$$

$$\sigma_f = \frac{\sigma_\theta - \sigma_r}{2\tau_p}\sigma_t, \quad \text{if} \quad \sigma_r < 0, \quad \frac{\sigma_\theta}{\sigma_r} > \beta,$$

where $\beta = (2\tau_p / \sigma_c - 1)/(2\tau_p / \sigma_t - 1)$.

For the arbitrary *r*, in the elastic stress field generated by explosion of concentrated charge, we have from (3)

$$N(r, t) = \frac{N_c}{t_0} \int_0^t \exp\left(\frac{\sigma_f(r, t - r)}{\sigma_0} \right) dt. \tag{7}$$

Relations (5)–(7) with the known potential $f(\xi)$ make it possible to calculate dynamics of damage accumulation in the elastic zone during explosion. Such process is readily realized for the elastic model at the initial stage when the elastic solution is valid in the domain $\alpha_0 \leq r \leq c_p t$. Defects

are the most intensively accumulated on the boundary of explosive cavity $a(t)$, and at a certain instant of time the defect density reaches its critical value N_c; then, the front of shattering wave $b(t)$ propagates into the medium. In order to establish further development of medium failure under the action of spherical charge explosion, it is required to consider joint movement of the medium failed and the elastic zone with the unknown $a(t)$ and $b(t)$.

Movement of the shattered rock was described by the motion equations of flowing medium and the Coulomb – Mohr law [3]. A distinctive feature of the model developed is the use of kinetic failure criterion according to which the concentration of defects in the elastic zone reaches the critical value of $N(z, t) = N_c$ at $z = b(t)$.

Differentiating this relation with respect to time, we have the following equation for the failure zone velocity:

$$\dot{b} = -\frac{\exp\dfrac{\sigma_f(b, t-b)}{\sigma_0}}{\displaystyle\int_{-1}^{t-b}\left[\frac{\partial}{\partial r}\left(\exp\frac{\sigma_f(r,\xi)}{\sigma_0}\right)\right]_{r=b} d\xi - \exp\frac{\sigma_f(b, t-b)}{\sigma_0}}, \tag{8}$$

where $\xi = t - r$.

Using (8) instead of (17) in system (15) – (19) [3], we obtain a complete system of ordinary differential equations for determining the elastic potential, as well as radii of explosion cavity and zone of shattering in the statement proposed.

As an example, let us present the concrete form of (8) when the first variant of the effective stress σ_f (5) is employed:

$$\dot{b} = \frac{1}{1 - \dfrac{\sigma_t}{\sigma_c\sigma_0 b^2}\displaystyle\int_{-1}^{t-b}\left(Af'' + \frac{2Bf'}{b} + \frac{3Bf}{b^2}\right)\exp\left(\frac{\sigma_f(b,\xi) - \sigma_f(b, t-b)}{\sigma_0}\right)d\xi},$$

$$\sigma_f(b,\xi) = \frac{\sigma_t}{\sigma_c}\left(-\frac{Af''}{b} - \frac{Bf'}{b^2} - \frac{Bf}{b^3} - P\alpha_2\right).$$

Here, $A = \alpha_2 - 2\mu^2 - 2\alpha_2\mu^2$, $B = -2\mu^2(3 + \alpha_2)$, and $\alpha_2 = \dfrac{\sigma_c}{\sigma_t} - 1$.

The system was solved by Euler's method. To describe the rock properties, the basic set of parameters was taken [3]: Young's modulus $E = 5\cdot10^{10}$ Pa, Poisson's ratio $\nu = 0.3$, and the density $\rho = 2500$ kg/m^3. The parameters of the friction law in the shattering zone were the following: $Y = 10^6$ Pa, $\alpha = 4$, $\sigma_c = 1.1\cdot10^8$ Pa, and $\sigma_t = 1.1\cdot10^7$ Pa. The rock pressure P was 10^5 Pa in calculations. The shear strength τ_p varied within the range $(0.5-2)\cdot10^9$ Pa. The pressure of explosive gases was assumed to change by the Jones – Miller adiabatic law with the initial pressure $p_0 = 1\cdot10^{10}$ Pa.

The constants of Eq. (1) for rocks are insufficiently studied. In this article, we used the parameters for organic glass from [4]: $\sigma_0 = (0.07-1.12)\cdot10^7$ Pa and $t_0 = 3.57\cdot10^{10}$ s. The value of N_c (determined by the rock structure) was taken as the unity of defect density. Note that N_c is not involved in the system of equations.

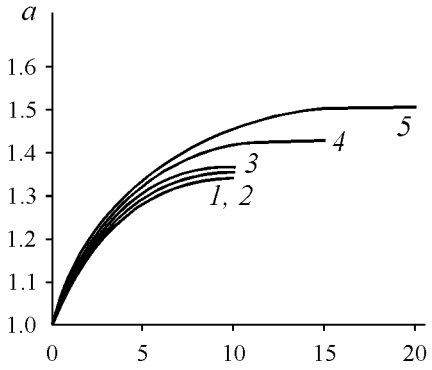

Fig. 2

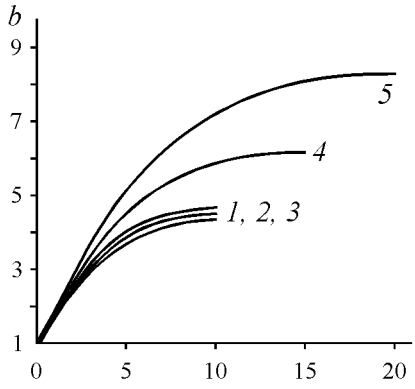

Fig. 3

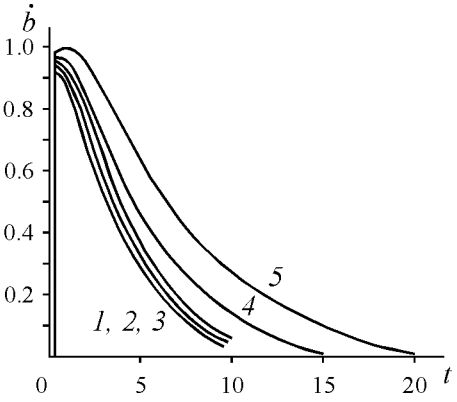

Fig. 4

The calculation results of expansion of the explosion cavity $a(t)$ and development of the shattering zone $b(t)$ and $\dot{b}(t)$ are shown in Figs. 2, 3, 4 (curves *1*–*5*) in the dimensionless coordinates: *1* and *2* correspond to the first and second variants of σ_f selection from (5) and (6), $\sigma_0 = 0.56 \cdot 10^7$ Pa, and $\tau_p = 1 \cdot 10^9$ Pa; *3* conforms to the static strength criterion [3] and $\sigma_c = 0.97 \cdot 10^9$ Pa; *4* and *5* correspond to the first variant of σ_f and $\sigma_0 = (0.28, 0.14) \cdot 10^7$ Pa. The rest of the parameters took the values from the basic set.

It is seen from the graphs that the choice of σ_f weakly affects $a(t)$ and $b(t)$. The change in σ_0 is more marked.

The proximity of curves *1*, *2* calculated from the damage accumulation model, and curve *3* obtained according to the approach [3] with the static criterion of Coulomb–Mohr type and specially selected σ_c turned out to be interesting. We succeeded in making such selection for all the variants of calculations performed with different values of σ_0, which is obvious from the data of Table 1. In its left part (columns 1–6), the parameters corresponding to the first variant of σ_f selection are given; the rest of the data are referred to the model [3] without damage accumulation. This proximity is explained by behavior of σ_f at the shattering wave front: the changes in its value within the time of failure development are fairly small. In Fig. 5, curves *1*–*3* depict the dependences of dimensionless radial, tangential, and effective stresses (at $r = b(t)$) on the time for $\sigma_0 = 0.56 \cdot 10^7$ Pa and $\tau_p = 1 \cdot 10^9$ Pa. The constancy of σ_f means that the failure condition [3] is satisfied at the front of shattering, and the selected value of the compressive strength σ_c is actually close to that one obtained from $\sigma_f : \sigma_f \sigma_c / \sigma_t$.

TABLE 1

σ_0, MPa	a_m	b_m	t_m	$\sigma_f \sigma_c / \sigma_t$, MPa	σ_f / σ_0	a_m	b_m	$Y_2 = \sigma_c$, MP
1	2	3	4	5	6	7	8	9
11.2	1.28	3.32	7.3	4355	38.89	1.29	3.32	4000
5.6	1.35	4.57	10.2	1931	34.48	1.36	4.58	1940
2.8	1.43	6.19	13.6	934	33.36	1.44	6.19	970
1.4	1.50	8.27	19.3	470	33.57	1.52	8.30	491
0.7	1.57	10.21	23.2	352	50.28	1.57	10.21	301

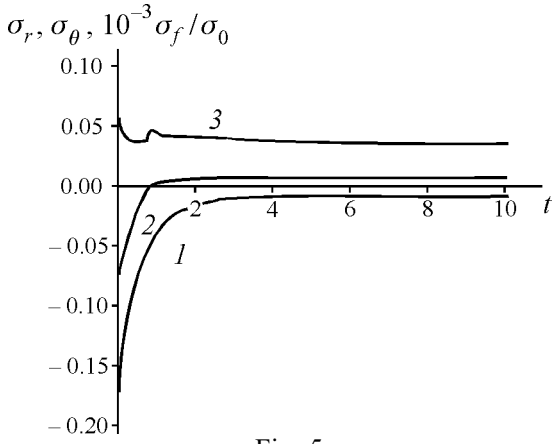

Fig. 5

Similarly to the behavior of $a(t)$ and $b(t)$, the dependences $\dot{b}(t)$ have mainly the same character except the initial stage of failure (Fig. 4). In this case, the influence of selecting the calculation variant of σ_f is evident. In the first variant (formula (5)), near the cavity, σ_f is small and even negative at the front of compression wave and initial stage of explosion. Hence, it appears that the influence exerted by the head part of the wave on the damage accumulation is insignificant, and failure of the cavity begins when σ_θ is positive. In the second variant (formula (6)), σ_f can be great at the wave front. Failure of the cavity can begin rapidly and develop with the maximum velocity. Then, due to stress drop in the wave, development of the shattering zone decelerates and accelerates again when σ_θ goes through 0. Figure 6 illustrates the dependences $\dot{b}(t)$ in the dimensionless form for different τ_p. Curves *1 – 4* correspond to the calculations with $\tau_p = 2;\ 1.5;\ 1;\ 0.5\cdot10^9$ Pa and $\sigma_\theta = 0.56\cdot10^7$ Pa. If τ_p is small, then shattering begins almost instantly with application of explosive load. When τ_p is great, failure occurs with a marked delay.

To determine a degree of rock disturbance in the elastic zone after cessation of the shattering wave, the calculations were performed for the relative density of the defects N at the points before the front of $b(t)$. The results are given in Table 2 ($\sigma_0 = 0.56\cdot10^7$ Pa and $\tau_p = 1\cdot10^9$ Pa).

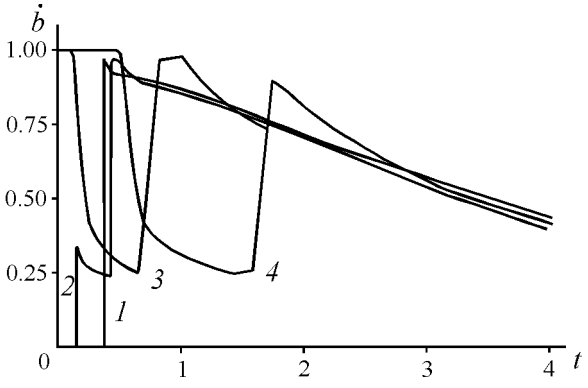

Fig. 6

TABLE 2

r	4.5	4.7	4.9	5.1
N (variant (5))	1	$3.2\cdot10^{-2}$	$1.7\cdot10^{-3}$	$1.3\cdot10^{-4}$
N (variant (6))	1	$3.7\cdot10^{-2}$	$2.2\cdot10^{-3}$	$2.0\cdot10^{-4}$

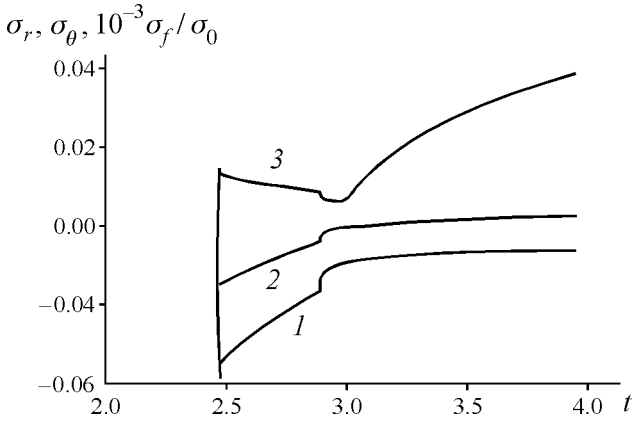

Fig. 7

It follows from Table 2 that as the distance from the explosion center increases, N decreases rapidly in the elastic zone; if N is equal to the critical density at the front at $r = 4.5a_0$, then when moving away to $0.2a_0$, it decreases by a factor of 30. The difference between the results of calculations for various selections of σ_f is small, which is explained by the unessential influence of the wave front on the damage accumulation as compared with the influence exerted by the stresses of the end part of the wave, where σ_θ reaches the great positive values. Curves *1 – 3* (Fig. 7) demonstrate the dependences of the radial, tangential, and effective stresses (in the dimensionless form) on the time at the point $r = 3.6a_0$ (the second line in Table 2). It is obvious from the graphs that at the wave front σ_f is less than its value at the shattering front almost by a factor of 2. Hence, due to the properties of exponential function, the value of integrand in (7) is less by a factor of 10^{10}, respectively.

CONCLUSIONS

The use of the long-term strength criterion in the problem on explosion gives the results close to the data obtained by the static criteria of strength.

Calculations of the defect density in the elastic region of explosion action showed that the defects concentrate mainly in the narrow zone of the order of the charge radius near the shattering front. Thus, it follows that the presence of disturbance observed in practice in the intact rock at great distances from the center of explosion cannot be explained by thermofluctuation mechanism of microcrack generation. This effect is conceivably connected with the rock-mass heterogeneity that was not taken into account in the model proposed.

REFERENCES

1. S. N. Zhurkov, “Kinetic concept of solid body strength. Thermofluctuation mechanism of failure,” *Vestn. AN SSSR*, No. 3 (1968).
2. A. N. Stavrogin and A. G. Protosenya, *Strength of Rocks and Stability of Workings at Great Depths* [in Russian], Nedra, Moscow (1985).
3. E. N. Sher and N. I. Aleksandrova, “Dynamics of breaking zone development during explosion of concentrated charge in a brittle medium,” *Fiz.-Tekh. Probl. Razrab. Polezn. Iskop.*, No. 5 (2000).
4. V. R. Regel’, A. I. Slutsker, and E. E. Tomashevskii, *Kinetic Nature of Strength of Solid Bodies* [in Russian], Nauka, Moscow (1974).